2018 25th International Lightning Detection Conference &
7th International Lightning Meteorology Conference
March 12 - 15 | Ft. Lauderdale, Florida, USA

A Detailed Look at the Performance Characteristics of the Lightning Imaging Sensor

Daile Zhang*, Kenneth L. Cummins
Department of Hydrology & Atmospheric Sciences
University of Arizona
Tucson, Arizona, USA
*dlzhang@email.arizona.edu

Philip Bitzer
Department of Atmospheric Science
University of Alabama in Huntsville
Huntsville, Alabama, USA

William J. Koshak
NASA Marshall Space Flight Center
Huntsville, Alabama, USA

***Abstract*— The Lightning Imaging Sensor (LIS) on board the Tropical Rainfall Measuring Mission (TRMM) effectively reached its end of life on April 15, 2015 after 17+ years of observation. Given the wealth of information in the archived LIS lightning data, and growing use of optical observations of lightning from space throughout the world, it is still of importance to better understand LIS calibration and performance characteristics. In this work, we continue our efforts to quantify the optical characteristics of the LIS pixel array, and to further characterize the detection efficiency and location accuracy of LIS. The LIS pixel array was partitioned into four quadrants, each having its own signal amplifier and digital conversion hardware. In addition, the sensor optics resulted in a decreasing sensitivity with increasing displacement from the center of the array. These engineering limitations resulted in differences in the optical emissions detected across the pixel array. Our work to date has shown a 20% increase in the count of the lightning events detected in one of the LIS quadrants, because of a lower detection threshold. In this study, we will discuss our work in progress on these limitations, and their potential impact on the group- and flash-level parameters.**

Keywords—Lightning Imaging Sensor; calibration; lightning detection

I. INTRODUCTION

Lightning observations from space have played a significant role in studying global thunderstorm and lightning activity [Boccippio et al., 2000; Christian et al., 2003; Cecil et al., 2014], as well as shedding light on application-related studies, such as lightning-produced NOx [Nesbitt et al., 2000; Bond et al., 2002; Murray et al., 2012], and the global electric circuit [Mach et al., 2011; Blakeslee et al., 2014a]. They have also improved our knowledge of thunderstorm evolution and detailed lightning activity within the thunderstorm lifecycle over both land and ocean by identifying the convective regions where the charging processes mainly occur.

One of the shortcomings of space optical observations, however, is the limited ability to determine the flash type for individual flashes, although statistical retrieval methods can be used to discriminate flash types based on the distributions of the mean optical characteristics [Koshak 2010; Koshak and Solakiewicz, 2015]. In addition, compared to most ground-based networks, space observations are known to have lower temporal and spatial resolution. In spite of these limitations, lightning observations from space have provided complementary information when compared to those obtained by the ground-based measurements and have become a critical tool for lightning studies.

The historical Lightning Imaging Sensor (LIS) ended its service in 2015 after 17 years of operation onboard the Tropical Rainfall Measuring Mission (TRMM) satellite [Christian et al., 1999, 2000]. Given the richness of the information, as well as TRMM LIS being a reference for the new Geostationary Lightning Mapper (GLM) and the second LIS instrument that is currently on the International Space Station (ISS LIS), it is important to understand the calibration performance of the TRMM LIS instrument and its optical characteristics.

The study is supported by NASA Cooperative Agreement 80MSFC17M0022.

Previous studies have reported on optical calibration [Boccippio et al., 2002; Koshak et al., 2000] and long-term stability [Buechler et al., 2014] of the LIS instruments. In this paper, we will examine the calibration of the LIS optical measurements and its impact on measured lightning parameters. A non-uniform behavior in the reported pixel energy density among the LIS pixel array quadrants and the reasons behind it are then discussed. This is followed by a 2-season assessment of the spatial offset in the LIS geo-registered centroid location of optical discharges (groups) as compared to lightning reports provided by the U.S. National Lightning Detection Network™ (NLDN).

II. Instrumentation and Methodology

A. Lightning Imaging Sensor

Using a 128×128 charge-coupled device (CCD) imager, LIS was designed to detect transient luminous radiation produced by both cloud-to-ground (CG) strokes and intra-cloud (IC) pulses. The spatial resolution of the CCD array was 4 km at nadir, decreasing somewhat towards the edges of the field-of-view (FOV). ISS LIS has an almost identical pixel footprint as TRMM LIS, as the ISS platform is operated at an altitude of 425 km, which is close to the TRMM altitude [Blakeslee et al., 2014b]. The LIS instruments detect the optical radiations emitted from lightning discharges in a very narrow band in the near infrared (777.4 nm) and identify lightning discharges during both daytime and nighttime [Christian et al., 1992; Boccippio et al., 2002; Chronis and Koshak, 2016] by using a dynamic background tracking technique. The incoming optical pulse energy on each pixel is then accumulated over an approximate 2 ms integration frame time with an uncertainty of 250 μs at the 95% confidence level [Bitzer and Christian, 2015], and the result is read out using a real-time processor that compares the optical energy of each pixel with the background illumination [Christian et al., 2003]. When the difference between the pixel signal in consecutive images exceeds a selected threshold based on the background image, the processor identifies this pixel as an LIS *event*, which is the most fundamental level in the LIS-reported data. It is possible that multiple optical pulses occurring within the frame integration time will contribute to one event [Mach et al., 2007]. Note that a LIS-defined event typically represents a small part of a lightning event/occurrence reported by ground-based measurements. In fact, less than 2% of LIS flashes consist of only one event. Note that an individual event in a multiple-event flash is not directly linked to a particular lightning discharge characteristics, and simply represents a lit-up pixel during the instrument frame integration time. Above-threshold detection of events in adjacent pixels during the frame integration time defines a LIS *group*, which can be physically associated with a CG stroke or a high-current "cloud pulse", and is frequently correlated with discharges reported by the NLDN (see II B). Once a group is identified, a group centroid is then geo-located by spatially weighting all the corresponding event locations by their radiance, representing the center of an optical pulse. Sufficiently close (in space and time) groups that occur within 330 ms and 5.5 km are accumulated into a LIS *flash* [Mach et al., 2007]. Likewise, a flash centroid is geo-located as a radiance-weighted location using all the included groups. Note that for each flash, LIS provides a product called "flash radiance." However, the flash radiance product defined for the Optical Transient Detector (OTD), and by extension the LIS instruments, is technically not flash radiance, but a spectral energy density, or "only a proxy to flash radiance" [see Appendix of Koshak 2010 for details]. But for simplicity, we may periodically use the term "radiance product" to identify the cumulative optical energy densities provided in this paper.

In addition to the direct lightning observations, the LIS instruments provide additional information every second to indicate the status of the instrumentation and the usability of the lightning data. It consists of 4 parameters, each of which is an 8-bit flag that depicts the status of the instrument, the satellite platform, external factors, and processing, with values of either "warning", "fatal" or "indifference" during that one second period [Boccippio et al., 1998; Christian et al., 2000]. Lightning data during the periods with a "fatal" flag and a selected subset of "warning" flags are not included in this study.

Overall, the model-predicted LIS flash detection efficiency of total lightning including cloud-to-ground (CG) and intra-cloud (IC) flashes was claimed to be 88%±9 initially [Boccippio et al., 2002], and afterwards validated as being between 70%-90% depending on the local time of day with the highest during the nights [Cecil et al., 2014].

B. U.S. National Lightning Detection Network

The ground-based lightning locating system – the U.S. National Lightning Detection Network™ (NLDN) uses a combined time-of-arrival/direction finding technology [Cummins et al., 1998] to geo-locate lightning discharges using roughly 100 LS7002 sensors uniformly covering the contiguous U.S. [Nag et al., 2014]. The detection efficiency of the NLDN has been evaluated by using various datasets including video observations [Biagi et al., 2007; Cummins et al., 2014; Zhang et al., 2015], tower data [Lafkovici et al., 2006, Cramer and Cummins, 2014], and triggered lightning data [Jerauld et al., 2005; Nag et al., 2011; Mallick et al., 2014]. The NLDN is able to discriminate CG and IC discharges with roughly 90% accuracy [Zhang et al., 2015; Zhu et al., 2016]. During the period of 2003 through 2012, it was expected to report 90-95% of all CG flashes, and some IC flashes (10-20%). In 2013 (mainly from April till August), the NLDN underwent a system-wide upgrade [Nag et al., 2014; Murphy and Nag, 2015], mainly focused on improving IC flash detection. Recent studies have shown an increased IC flash detection efficiency to 45-60% after this upgrade [Murphy and Nag, 2015].

When a lightning discharge is detected, the NLDN reports the discharge with the primary information of its time (accurate to the microsecond), location, peak current and discharge type (IC or CG). Additionally, the NLDN clusters the discharges into flashes based on its grouping algorithm described in Murphy and Nag, [2015]. An NLDN discharge (either a cloud pulse or a ground stroke) is essentially equivalent to a LIS group, not a single LIS event. To be more precise, we will use "group-level" to indicate the analysis between LIS groups and NLDN-reported discharges. Given

that a LIS event is a single "lit-up" pixel in a 2 ms time period, and has no equivalent structure in an NLDN report, LIS events are not considered in the inter-comparison analysis.

III. Results and Discussions

A total of 141,871,664 LIS events were collected during two years of TRMM LIS observations (2012 and 2013), comprising 31,983,244 groups and 2,868,097 flashes. All of the data were used for the evaluation study of the LIS optical characteristics. Due to the data availability, however, data from the summer months (June-July-August) were analyzed for the study of the LIS group-centroid location offsets.

A. Pixel Energy Density

Fig 1 summarizes the performance behaviors of the pixel thresholds, count of events detected, total energy density, and mean energy density. Since the LIS focal plane is divided into four quadrants with somewhat different sensitivities, both event count and mean energy density showed an obvious contrast in the top-left quadrant (Q1) compared to the other three. This inconsistency in the LIS focal plane was caused by a compromise of the LIS design that could not be mitigated using the 1990s technology. The LIS CCD was read out as four quadrants, with each having its own signal amplifier and digital conversion hardware, and the four outputs were then combined into a single data stream before further processing. The threshold of event energy density in the top-right (Q1), top-left (Q2), bottom-left (Q3), and bottom-right (Q4) quadrants were 2.866, 3.602, 3.489 and 3.349 μJ m^{-2} $ster^{-1}$ nm^{-1}, respectively, as shown in Fig. 1(a). Due to the lower threshold in Q1, it was more sensitive and consequently reported roughly 20% more lightning occurrences with lower energy being detected, compared to the other quadrants. Although this quadrant sensitivity inconsistency did not have a big impact on flash detection efficiency because of the LIS flash clustering algorithm (LIS flashes with only one event only consist of 2% of all the data), it certainly had an impact on the event- and group- level detection efficiencies, as well as group parameters, which will be discussed in the next section. For the mean energy densities shown in Fig. 1(d), Q1 had lower values overall, as the lower threshold allowed many more lower-energy events to be detected in the quadrant. However, this inter-quadrant non-uniformity shows little or no effect on the total energy density values, as shown in Fig. 1(c), since Q1 detected more lower-energy events, as opposed to less high-energy events, which contributed little to the overall totals.

The pixel maximum energy density (which in conjunction with the threshold, determines each's pixel dynamic range) varies among the quadrants (not shown). A roughly 40% higher maximum-energy density value was detected in Q1, as shown in the histogram in Fig. 2. Since these large-energy events are only made up of a very small fraction of the total events, it did not have a large impact on the quadrant mean energy density. Moreover, the dynamic ranges in the other quadrants were somewhat different. For instance, although Q4 has the second lowest threshold, Q4 has the shortest dynamic range, as no events with energy density exceeded 500μJ m^{-2} $ster^{-1}$ nm^{-1} were detected. It is possible that these maximum energy density values are compromised by the limited number of observations, since they are the extreme values within the dataset.

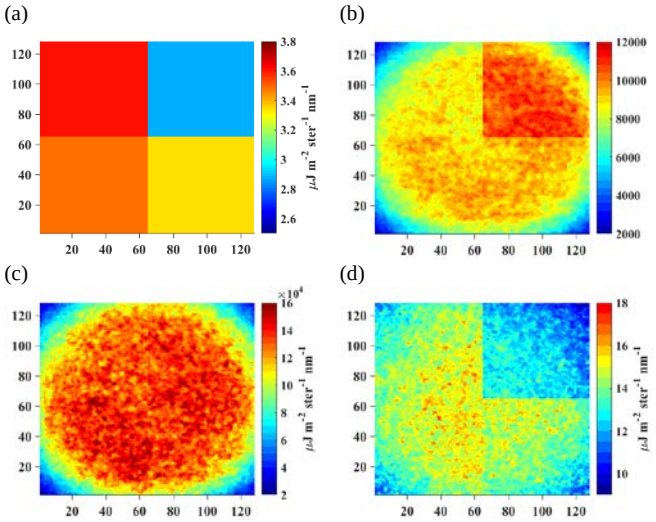

Fig. 1 Characteristics of (a) Minimum threshold event energy detected, (b) Number of events detected, (c) Total event energy density, and (d) Mean event energy density

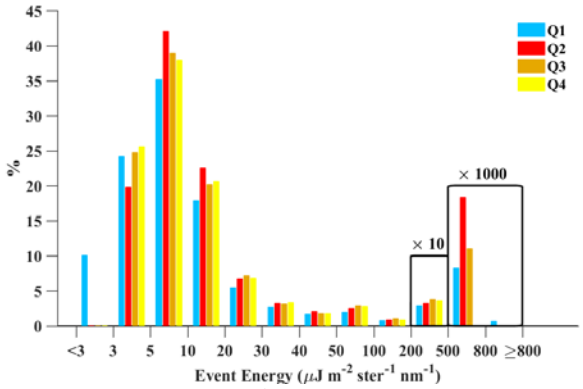

Fig. 2 Histogram of LIS event energy density

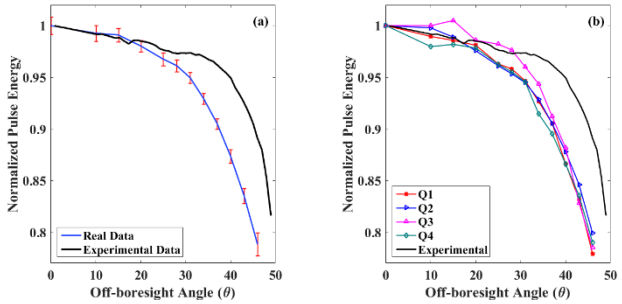

Fig. 3 (a) Event mean energy density, and (b) Quadrant event mean energy density fall-off with off-boresight angle

Due to the fact that the LIS pixel array was designed to receive incoming photons from lightning pulses, scattered

somewhat by intervening clouds, the total event energy density received at each pixel is a function of the optical geometry. This is illustrated in Fig. 1(c), which shows a radially-symmetric fall-off in mean event energy density with increasing distance from the center of the array. Laboratory calibration tests have shown that the detected normalized pulse energy density experienced an exponentially decrease with the increasing off-boresight angle from the aperture center [Boccippio et al., 2001]. A similar decrease pattern can also be derived from our 2-year mean event energy density dataset, as shown in Fig. 3(a). The mean values have been normalized to a maximum value of 1 near the boresight ($\theta = 0$). For each individual quadrant, this similar decreasing pattern is within 2-3% variabilities below 35 degree due to the limited sample size (see Fig. 3(b)). It is obvious that the response function derived from our 2-year normalized data experiences an 8-10% more rapid decrease than those from the previous laboratory-calibrated data (black curve) beyond 20° off-boresight angle. Our preliminary hypothesis is that the rapid fall-off rate has nothing to do with the instrument, but rather a cloud optical attenuation effect. Since the off-boresight angle fall-off correction had not been implemented with OTD, TRMM LIS, or ISS LIS, this deviation in the mean energy density will largely influence our previous understanding of the LIS pixel array optical characteristics, as well as effectively setting of the transient thresholds.

B. Group Energy and Group Areas

Based on the event-group clustering algorithm [Mach et al., 2007], a LIS group is consist of one or more adjacent (neighboring or diagonal) pixels that are illuminated as events in the pixel array during the same 2 ms frame time. The difference in the dynamic range, especially the minimum threshold of the four quadrants, has the potential cause an inconsistency in the group parameters, such as group energy and group footprint (equivalent to group area). To explore this possibility, the group areas (GA) and group energy density (GR) were evaluated as follows.

For this group-level analysis, we considered the groups with all the corresponding events in a single quadrant as being associated with that quadrant. The groups having event pixels in more than one quadrant were defined as "Multiple", and these groups were frequently larger than the single-quadrant groups. Frequency histograms for the count of GA and GR were produced for the 5 group categories and are shown in Fig. 4. The average GA in Q1 in both years is roughly 20% greater than for Q3 and Q4, and 15% greater than for Q2. The normalized GA histograms in Fig. 4(a) clearly show that Q1 has higher fractional values (more-frequent occurrence) greater than 100 km^2 than the other quadrants, whereas other three quadrants show a higher fraction for GAs that are smaller than 200 km^2. Notably, GA fractions in "Multiple" show even higher values in the larger GAs than Q1, which is consistent with the nature of groups pervading multiple quadrants.

The fact that the groups in Q1 are statistically larger than those of other quadrants is related to the fact that more events with lower energy density are detected in Q1. These lower-energy events usually lie on the edges of a group; hence, they act to increase the size of the group. Additional evidence comes from the ratio of events to groups. The average ratios in each quadrant (1 through 4) are 5.1, 4.4, 4.2, and 4.3, respectively. Thus, there are roughly more 0.8 pixels (events) on average that occur in Q1. These extra pixels can only be on the edges of the groups. Also shown in Fig. 4(c), Q1 has higher percentages of groups with more than 5 events than those in the other three quadrants. For "Multiple" quadrant groups, the ratio is even higher and can even be more than 200.

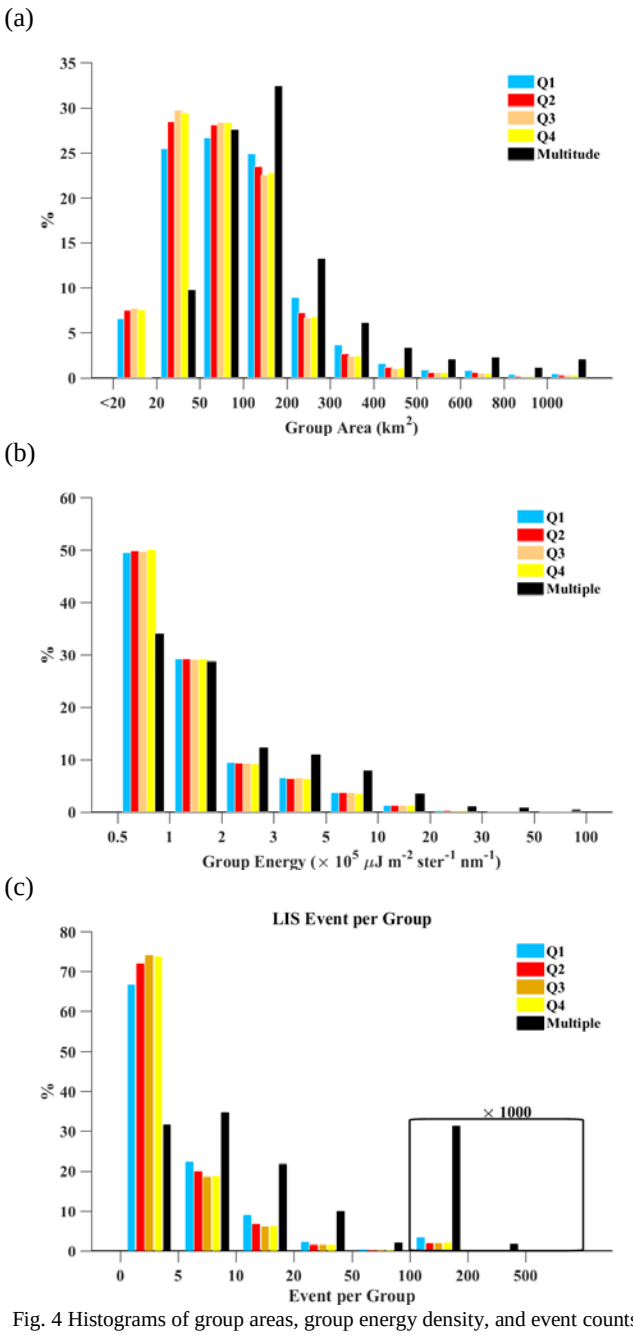

Fig. 4 Histograms of group areas, group energy density, and event counts per group

On the other hand, the mean group energy density in Q1 does not show a huge difference when compared to the other

three quadrants. As defined in the Algorithm Theoretical Basis Document for the LIS [Christian et al., 2000], a group energy is the "calibrated total energy of all the events associated with the group." Even though groups in Q1 tend to have more pixels/events, their energy density associated with these additional pixel is low, having little impact on the total energy density. Interestingly, the mean group energy in "multiple" quadrants is almost four times larger than those in a single quadrant. Our interpretation is that in order for a group to occupy multiple quadrants, not only does it have to be spatially larger, but also it has to be more intense, resulting in higher optical energy. In other words, optically intense lightning discharges tend to be spatially larger. The statistics of the maximum event energy in the group further illustrates that the average maximum event energy in multiple quadrants is more than two times of those in a single quadrant. From all the results above, it is clear that the distinction of the pixel sensitivity in the LIS pixel array has noticeable impacts on the group parameters.

C. LIS Group Centroid Location

Previous studies [Thomas et al., 2000; Rudlosky, et al., 2013; Rudlosky, 2015; Rudlosky et al., 2017] have shown that there is a location offset of the LIS group centroid, relative to the location of time-coincidence discharge observed by various ground-based measurements. As discussed in our previous ILDC paper [Zhang et al., 2016], these average location offset are around 5-6 km, which is the length about 1-1.5 LIS pixels. We also reported a transition pattern in the north:south direction of these offsets (NLDN location minus LIS group centroids in the analysis) at some specific times, when the TRMM satellite performed 180 degree yaw maneuvers, which were designed to shade the instruments from solar radiation and occurred every 15-20 days when the satellite at the position to prevent the direct sunlight on the onboard instruments. During the two periods studied in that paper, two 180 degree yaw maneuver operations occurred. Comparing to the behaviors of the LIS group centroid offsets before and after the yaw maneuver, we concluded that the TRMM operations of yaw maneuver have led to a location bias in LIS observations, and this bias can and should be corrected based on the date, time and direction of the TRMM operations (The full operational information including date, time and orbit number for the 180 degree TRMM yaw maneuvers are available at: http://www.eorc.jaxa.jp/en/hatoyama/satellite/satdata/maneuver/Yaw_e.pdf.). A simple but effective correction method was also proposed in the study to improve the location accuracy of LIS group level data, as shown in Fig 5. An individual LIS group centroid can be adjusted by adding or distracting 5 km (average location bias, about one LIS pixel size) to the original data in the latitudinal direction depending on the direction of the TRMM yaw maneuver. For south-bias days, 5 km is added to the latitudes of all the time-matched LIS group centroids, while for north-bias periods, 5 km is subtracted from the latitudes of all the time-matched LIS group centroids.

In this study, we have expanded our dataset to two summers to further investigate the behavior of the LIS location offsets and verify our previously-proposed correction method. During our studied period, TRMM performed 31 times of yaw maneuver operations (16 times in 2012 and 15 times in 2013), which led to 32 times of transitions. The results show that the original LIS location offsets without correction exhibited a 4-6 km bias in both years, illustrated by the two frequent occurrence (yellow) regions in the 2-dimensional histogram in Fig. 5 (a). Of the 54,705 group centroid bias samples that were collected and used in the calculation, 24,892 were positive as LIS biased to the south while 29,813 were negative as LIS biased to the north. The two-year average mean (median) positive offsets was 5.80 (5.20) km, and -6.76 (-6.34) km for the negative offsets. Note that there is less than 2% difference in the mean and median values between the two years, which shows a consistency of the offsets over the time. By applying our previously-proposed correction method to all the time-matched LIS group centroids during the studied period, it is obvious that LIS group centroids matched better with the NLDN locations in space, as shown in the 2-D histogram in Fig. 5 (b). The mean (median) of the location offsets with correction in the latitudinal direction during the two summers (regardless of signs) was 3.61 (2.52) km, with 3.43 km as the standard deviation. Also notice that similar to our previous results [Zhang et al., 2016], the mean bias in the location offsets are mainly in the latitudinal direction. The bias in the longitudinal direction is negligible comparing to the bias in the latitudinal direction in both years. A comparison of the LIS group centroids with the global Earth Networks Total Lightning Network (ENTLN) showed similar results [Bitzer, personal communication]. Therefore, it is recommended that this simple method be used for correcting LIS group centroids for inter-comparison studies involving other geo-located datasets.

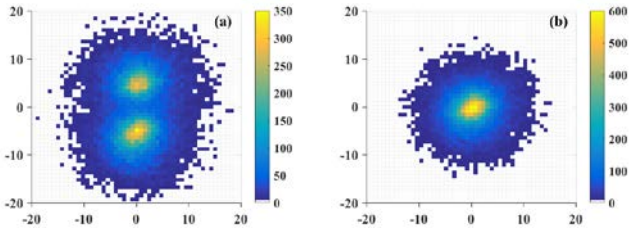

Fig. 5 LIS group-centroid location offsets compared to time-matched NLDN discharges (a) without correction, and (b) with correction

LIS location offsets could also vary as a function of latitude and longitude. As shown in Fig. 6 (a), there is no significant difference in the location offsets with respect to latitudes between 32-36° N, whereas a slight increase in the location offsets with increasing latitude is seen beyond 36° N. This phenomenon may be due to the increasing LIS pixel size at the edges of the focal plane. Consequently, to correct those LIS groups detected at higher latitudes, a number than 5 km might need to be used. In addition, there is some variation of the location offsets below 36° N. These variations came from individual storms on different days. Notice a clear pattern of 4 km offsets between 33.2 and 33.4 degrees in Fig. 6(a), which is solely caused by a mesoscale system on July 24th, 2013 sweeping across Texas, Arkansas, and Louisiana, leading to a few hundred millions of CG strokes and IC pulses according to the NLDN reports. As stated in the previous paragraph, a specific correction distance number should be applied for daily analysis. For the sake of simplicity, and especially when the

studied period is longer than a few TRMM transition periods, 5 km is still a good estimation. In general, the longitudinal offsets (regardless of signs) show a slight decrease from the east to the west over the continental U.S. It is probably related to the geographical difference in lightning occurrence. The mean (median) of the longitudinal offsets during the two years is 3.61 (2.55) km, which is comparable to the latitudinal offsets with corrections.

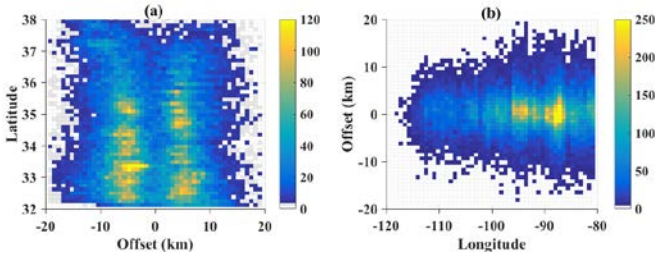

Fig. 6 LIS group-centroid location offsets variation with (a) latitudes, and (b) longitudes

IV. Conclusions

In this study, LIS optical characteristics are evaluated using two years of data throughout the full TRMM orbit. The LIS group-centroid location offsets are also compared over continental U.S. with the NLDN data. The conclusions are as follows:

1) An inconsistency of the mean event (pixel) energy density in the LIS pixel array is found among the four independent quadrants. The threshold of the event energy density in the four quadrants varies, which has led to statistically meaningful differences in the mean energy density and the counts of events detected. This is due to the engineering limitation from the 1990s technology where the LIS CCD was read out as four quadrants and had various sensitivities. The quadrant with the lowest threshold has led to an approximate 20% increase in the count of events being detected and roughly 20% decrease in the mean event energy.

2) There is a fall-off pattern in the mean event energy density in the entire LIS pixel array as the off-boresight angle increases. Similar patterns are found in all four individual quadrants. These patterns differ from the laboratory results in that they show a 8-10% more rapid fall rate beyond 15 degrees. This difference may result from a longer in-cloud diffusion path with increasing off-boresight angle, and this possibility will be explored in future work. This would not be an instrumentation issue, but rather a cloud attenuation effect.

3) The quadrant with the lowest threshold (Q1) showed a 20% larger groups than other quadrants, as more events on the edges of the groups with lower energy can be detected in that quadrant. Groups extended to multiple quadrants contain more events than groups that those constrained to be in a single quadrant, and are frequently more intense.

4) Our 5 km correction method for the LIS group-centroid location offsets that were caused by TRMM 180 degree yaw manuever has been tested using more data and has proved to be effective. The LIS location offsets in the longitude direction are much smaller than in the latitude direction, and is statistically insignificant. The variation of the LIS location offsets as a function of longitude is neglegible, whereas the location offsets as a function of latitude shows an increase beyond 36 degree, and it is probably owing to the distortion of the LIS pixel size on the edges of the focal plane.

Acknowledgment

The authors would also like to thank the Global Hydrology Resource Center (GHRC) and Vaisala Inc. for providing the LIS data and the NLDN data, respectively. Discussions about LIS design and implications with Drs. Dennis Buechler and Hugh Christian are also appreciated.

References

Bitzer, P. M., and H. J. Christian (2015), Timing uncertainty of the lightning imaging sensor, Journal of Atmospheric and Oceanic Technology 32, no. 3: 453-460.

Bond, D. W., S. Steiger, R. Zhang, X. Tie, and R. E. Orville (2002), The importance of NO x production by lightning in the tropics, Atmospheric Environment 36, no. 9: 1509-1519.

Blakeslee, R. J., D. M. Mach, M. G. Bateman, and J. C. Bailey (2014a), Seasonal variations in the lightning diurnal cycle and implications for the global electric circuit, Atmospheric research 135: 228-243.

Blakeslee, R. J., H. J. Christian, M. F. Stewart, D. M. Mach, M. Bateman, T. D.Walker, D. Buechler, W. J. Koshak, S. OBrien, T. Wilson, and E. C. Colley (2014b), Lightning Imaging Sensor (LIS) for the International Space Station (ISS): mission description and science goals.

Boccippio, D.J. and H. J. Christian (1998), Optical detection of lightning from space, NASA Technical Report.

Boccippio, D. J., S. J. Goodman, and S. Heckman (2000), Regional differences in tropical lightning distributions, Journal of Applied Meteorology 39, no. 12: 2231-2248.

Boccippio, D.J., K. L. Cummins, H. J. Christian, and S. J. Goodman (2001), Combined satellite-and surface-based estimation of the intracloud–cloud-to-ground lightning ratio over the continental United States, Monthly Weather Review, 129(1), pp.108-122.

Boccippio, D. J., W. J. Koshak, and R. J. Blakeslee (2002), Performance assessment of the optical transient detector and lightning imaging sensor. Part I: Predicted diurnal variability, Journal of Atmospheric and Oceanic Technology 19, no. 9: 1318-1332.

Buechler, D. E., W. J. Koshak, H. J. Christian, and S. J. Goodman (2014), Assessing the performance of the Lightning Imaging Sensor (LIS) using deep convective clouds, Atmospheric research, 135, pp.397-403.

Cecil, D. J., D. E. Buechler, and R. J. Blakeslee (2014), Gridded lightning climatology from TRMM-LIS and OTD: Dataset description, Atmospheric Research 135: 404-414.

Christian, H. J., R. J. Blakeslee, and Steven J. Goodman (1992), Lightning imaging sensor (LIS) for the earth observing system, NASA Technical Reports.

Christian, H. J., R. Blakeslee, S. Goodman, D. Mach, M. Stewart, D. Buechler, W. Koshak, J. M. Hall, W. L. Boeck, K. T. Driscoll, and D. J. Boccippio (1999), The lightning imaging sensor, NASA conference publication, pp. 746-749. NASA.

Christian, H. J., R. J. Blakeslee, S. J. Goodman, and D. M. Mach (2000), Algorithm theoretical basis document for the lightning imaging sensor, NASA Earth Science Department Technical Report.

Christian, H. J., R. J. Blakeslee, D. J. Boccippio, W. L. Boeck, D. E. Buechler, K. T. Driscoll, S. J. Goodman, J. M. Hall, W. J. Koshak, D. M. Mach, and M. F. Stewart (2003), Global frequency and distribution of lightning as observed from space by the Optical Transient Detector, Journal of Geophysical Research: Atmospheres 108, no. D1.

Chronis, T., and W. J. Koshak (2016), Diurnal Variation of TRMM/LIS Lightning Flash Radiances, Bulletin of the American Meteorological Society.

Cummins, K. L., M. J. Murphy, E. A. Bardo, W. L. Hiscox, R. B. Pyle, and A. E. Pifer (1988), A combined TOA/MDF technology upgrade of the US National Lightning Detection Network, Journal of Geophysical Research: Atmospheres 103, no. D8: 9035-9044.

Koshak, W. J., M. F. Stewart, H. J. Christian, J. W. Bergstrom, J. M. Hall, and R. J. Solakiewicz (2000), Laboratory calibration of the optical transient detector and the lightning imaging sensor, Journal of Atmospheric and Oceanic Technology17, no. 7: 905-915.

Koshak, W. J (2010), Optical characteristics of OTD flashes and the implications for flash-type discrimination, Journal of Atmospheric and Oceanic Technology 27, no. 11: 1822-1838.

Koshak, W. J., and R. J. Solakiewicz (2015), A method for retrieving the ground flash fraction and flash type from satellite lightning mapper observations, Journal of Atmospheric and Oceanic Technology 32, No. 1: 79-96.

Mach, D. M., H. J. Christian, R. J. Blakeslee, D. J. Boccippio, S. J. Goodman, and W. L. Boeck (2007), Performance assessment of the optical transient detector and lightning imaging sensor, Journal of Geophysical Research: Atmospheres 112, no. D9.

Mach, D. M., R. J. Blakeslee, and M. G. Bateman (2011), Global electric circuit implications of combined aircraft storm electric current measurements and satellite‐based diurnal lightning statistics, Journal of Geophysical Research: Atmospheres 116, no. D5.

Murphy, M. J., A. Nag, J. A. Cramer, and A. E. Pifer (2014), Enhanced cloud lightning performance of the US National Lightning Detection Network following the 2013 upgrade, 23rd International Lightning Detection Conference & 5th International Lightning Meteorology Conference, pp. 18-21.

Murray, L. T., D. J. Jacob, J. A. Logan, R. C. Hudman, and W. J. Koshak (2012), Optimized regional and interannual variability of lightning in a global chemical transport model constrained by LIS/OTD satellite data, Journal of Geophysical Research: Atmospheres 117, no. D20.

Nag, A., M. J. Murphy, K. L. Cummins, A. E. Pifer, and J. A. Cramer (2014), Recent evolution of the us National lightning detection network, In Preprints, 23rd Int. Lightning Detection Conf., Tucson, AZ.

Nag, A., M. J. Murphy, W. Schulz, and K. L. Cummins (2015), Lightning locating systems: Insights on characteristics and validation techniques, Earth and Space Science 2, no. 4: 65-93.

Nesbitt, S. W., R. Zhang, and R. E. Orville (2000), Seasonal and global NOx production by lightning estimated from the Optical Transient Detector (OTD), Tellus B 52, no. 5: 1206-1215.

Rudlosky, S. D., and D.T. Shea (2013), Evaluating WWLLN performance relative to TRMM/LIS, Geophysical Research Letters 40, no. 10: 2344-2348.

Rudlosky, S. D (2015), Evaluating ENTLN Performance Relative to TRMM/LIS, Journal of Operational Meteorology 3, no. 2.

Rudlosky, S. D., M. J. Peterson, and D. T. Kahn (2017), GLD360 Performance Relative to TRMM/LIS, Journal of Atmospheric and Oceanic Technology.

Thomas, R. J., P. R. Krehbiel, W. Rison, T. Hamlin, D. J. Boccippio, S. J. Goodman, and H. J. Christian (2000), Comparison of ground‐based 3‐dimensional lightning mapping observations with satellite‐based LIS observations in Oklahoma, Geophysical research letters 27, no. 12: 1703-1706.

Zhang, D., K. L. Cummins, and A. Nag (2015), Assessment of cloud lightning detection by the U.S. National Lightning Detection Network using videos and Lightning Mapping Array observations, AMS Conference, Phoenix, AZ.

Zhang, D., K. L. Cummins, A. Nag, M. Murphy, and P. Bitzer (2016), Evaluation of the National Lightning Detection Network Upgrade Using the Lightning Imaging Sensor, International Lightning Detection Conference, San Diego, CA.

Zhu, Y., V. A. Rakov, M. D. Tran, and A. Nag (2016), A study of National Lightning Detection Network responses to natural lightning based on ground truth data acquired at LOG with emphasis on cloud discharge activity, Journal of Geophysical Research: Atmospheres, 121(24).